

Serveur Académique Lausannois SERVAL serval.unil.ch

Author Manuscript

Faculty of Biology and Medicine Publication

This paper has been peer-reviewed but does not include the final publisher proof-corrections or journal pagination.

Published in final edited form as:

Title: Negative control of CSL gene transcription by stress/DNA damage response and p53.

Authors: Menietti E, Xu X, Ostano P, Joseph JM, Lefort K, Dotto GP

Journal: Cell cycle (Georgetown, Tex.)

Year: 2016 Jul 2

Volume: 15

Issue: 13

Pages: 1767-78

DOI: 10.1080/15384101.2016.1186317

In the absence of a copyright statement, users should assume that standard copyright protection applies, unless the article contains an explicit statement to the contrary. In case of doubt, contact the journal publisher to verify the copyright status of an article.

Negative control of CSL gene transcription by stress / DNA damage response and p53

Elena Menietti¹, Xiaoying Xu¹, Paola Ostano², Jean-Marc Joseph³, Karine Lefort^{1,4*} and G. Paolo Dotto^{1,5*}

¹ Department of Biochemistry, University of Lausanne, Epalinges, CH-1066, Switzerland;

² Cancer Genomics Laboratory, Edo and Elvo Tempia Valenta Foundation, Biella, 13900, Italy;

³ Pediatric surgery Department, University Hospital CHUV, CH-1011 Lausanne, Switzerland.

⁴ Department of Dermatology, University Hospital CHUV, Lausanne, CH-1011, Switzerland.

⁵ Cutaneous Biology Research Center, Massachusetts General Hospital, Charlestown, MA 02129, USA;

*Co-corresponding authors: paolo.dotto@unil.ch; karine.lefort@unil.ch

Conflicts of interest

The authors declare that no conflicts of interest exist.

Abbreviations

HDFs: Human Dermal Fibroblasts

CAFs: Cancer Associated Fibroblasts

ROS: Reactive Oxygen Species

UVA: Ultra Violet A

RCA/CCP: Regulators of Complement Activation/ Complement Control Proteins.

Abstract

CSL is a key transcriptional repressor and mediator of Notch signaling. Despite wide interest in CSL, mechanisms responsible for its own regulation are little studied. CSL down-modulation in human dermal fibroblasts (HDFs) leads to conversion into cancer associated fibroblasts (CAF), promoting keratinocyte tumors. We show here that CSL transcript levels differ among HDF strains from different individuals, with negative correlation with genes involved in DNA damage/repair. CSL expression is negatively regulated by stress/DNA damage caused by UVA, Reactive Oxygen Species (ROS), smoke extract, and doxorubicin treatment. P53, a key effector of the DNA damage response, negatively controls CSL gene transcription, through suppression of CSL promoter activity and, indirectly, by increased p21 expression. CSL was previously shown to bind p53 suppressing its activity. The present findings indicate that p53, in turn, decreases CSL expression, which can serve to enhance p53 activity in acute DNA damage response of cells.

Keywords: CSL/RBPJ κ , dermal fibroblasts, individual variations in gene transcription, UVA/DNA damage response, p53

Introduction

CSL (CBF1, SUH, Lag1, also known as RBPJ κ) is a highly conserved transcription factor with both Notch dependent and independent roles. ¹ This DNA binding protein is endowed with intrinsic transcription repressive function, and is converted into an activator of transcription by association with the proteolytically cleaved activated forms of Notch receptors. CSL binds to regulatory regions of target genes in a dynamic and cell-type specific manner, and genes to which it binds with high affinity can be similarly induced by CSL down-modulation and Notch activation. ¹ We have recently showed that CSL expression in dermal fibroblasts is key for skin homeostasis, and that its down-modulation results in a cancer-inducing stromal environment. ² Loss of CSL gene function leads to the conversion of dermal fibroblasts into cells with cancer associated fibroblast (CAF) properties, with subsequent recruitment of inflammatory cells and establishment of « *cancer fields* », with expanding premalignant and malignant keratinocytic lesions. ^{2,3} The *in vivo* significance of these findings is supported by the fact that CSL is less expressed in stromal fibroblasts of premalignant and malignant skin SCC lesions relative to surrounding normal skin. ⁴ However, the mechanisms involved in CSL down-regulation remain to be investigated.

Surprisingly little is known on control of CSL gene expression. The Notch pathway is built on a series of positive and negative feedback loops often operating in a cell type-specific manner. ⁵ This complex mode of regulation results from convergent and reciprocal control of expression of the canonical components: Notch ligands, Notch receptors, CSL, and transcriptional repressors of the Hes/Hey family, as well as co-factors like

MAML proteins.⁵ The *Drosophila melanogaster* and *Caenorhabditis elegans* homologs of CSL, Suppressor of Hairless (SuH) and LAG-1 respectively, can either activate or repress their own expression, determining cell fate.^{6,7} Little else is known of control mechanisms of CSL gene transcription. At the protein level, other pathways converge on control of its function. For instance, in mammalian cells Wnt signaling can inhibit CSL activity by direct binding of Dishevelled, and CSL stability is regulated by Presenilin-2 and p38 MAP-kinase, while its cellular localization can be regulated in *Xenopus laevis* or mammalian cells by RITA or SMRT protein complexes.⁸⁻¹¹

Recent advances in human genomic and transcriptomic analyses provide insights into individual differences in susceptibility to disease, with tissue-specific control of gene expression as key determinant.¹² For novel insights into control of CSL gene expression, we started from the study of individual variations in gene expression in human dermal fibroblasts (HDFs) derived from many different individuals. Gene ontology analysis of co-regulated genes pointed to the DNA damage / stress response as a possible negative regulator of CSL expression, which we experimentally assessed in HDFs upon various treatments. Importantly, we found that p53, a key element in the DNA damage / stress response, is involved in negative control of CSL transcription by direct binding to the CSL gene and/or through its effector p21. The Notch and p53 pathways interact at multiple levels, in a context dependent manner.¹³ We recently uncovered that, in HDFs, CSL functions as a direct negative regulator of p53 activity and that induction of p53-dependent cellular senescence provides a fail-safe mechanism against the consequences of compromised CSL activity.⁴ The present findings indicate

that p53, in turn, represses CSL transcription, which can serve to enhance p53 activity in the acute response of cells to DNA damaging cancer-threatening conditions.

Results

1) Individual variations in Notch/CSL signaling genes

Substantial differences can exist in levels of gene expression among cells from different individuals that are key to understand variations in susceptibility to disease.¹² As mentioned, CSL plays an important role in dermal fibroblasts as negative regulator of senescence and CAF activation.^{2, 4} To probe into individual variations in expression of CSL and related genes, we undertook RNA sequencing analysis of second passage HDFs derived from 46 healthy individuals (GSE77371 and Supplementary Table 1). RNA sequencing reads showed that, besides CSL (Fig. 1A), several components of the Notch family are expressed at significant levels in HDFs, with NOTCH2 being more highly expressed than NOTCH1 as we previously reported² (Fig. 1B). Among Notch ligands, JAG1 expression was greater than DLL1 (paired t-test $p < 0.0001$), while JAG2, DLL2 and DLL4 expression was not detectable (Fig. 1C). Among canonical Notch/CSL targets, HES4 was more expressed than HES1 or HES6 (paired t-test $p < 0.0001$), with HES1 being expressed only in some strains (38/46) (Fig. 1D). Comparative RT-qPCR and RNA-seq analysis of lowly expressed genes like DLL1 in a selected set of samples showed comparable individual variations (Fig. 1E). CSL expression was modulated around a RPKM average of 9.8, with higher levels being found in some HDF strains and lower in others (CV, coefficient of variation of 0.26) (Fig. 1A). Two other

genes, NOTCH3 and JAG1, showed high heterogeneity of expression among the various strains (CV > 0.6), while NOTCH2 was highly expressed in all, with very little variation (CV = 0.15) (Fig. 1B, C).

Notch signaling components have the potential of controlling each other's expression in either a positive or negative fashion.^{5, 14} Correlation analysis of RNA-seq data showed that CSL levels among various cell strains were inversely regulated with those of NOTCH1, consistent with CSL functioning as a repressor of this gene⁵, while CSL expression was positively correlated with DLL1 and TLE1, suggesting common control mechanisms (Fig. 1F). Interestingly, a trend of positive and negative correlation between expression of CSL and other Notch signaling components was also observed (Fig. 1F). Although not statistically significant, this was confirmed by RT-qPCR (Fig. 1G). Among the inversely related genes we note HES1, which we previously showed to be up-regulated in HDFs by CSL silencing.⁵

2) Identification of CSL-coregulated genes

We recently showed that down-modulation of CSL expression leads to fibroblast senescence, with the concomitant induction of a CAF phenotype.⁴ Consistent with these findings, CSL expression was overall inversely correlated to that of CAF effector genes with WNT3, PKM and NGF showing the best Pearson scores ($p < 0.005$) (Fig. 1H).

For more general insights into CSL regulation and function, we broadened our analysis of the RNA-seq profiles for identification of all genes significantly correlated with CSL in either a positive or negative manner. Expression of 466 genes was positively correlated with that of CSL across the

46 strains, (Pearson score > 0.5 , $p < 0.0005$), while 576 genes were negatively correlated (Pearson score < -0.5 , $p < 0.0005$) (Fig. 1I and Supplementary Table 2). Gene ontology and pathway analysis showed that genes positively correlated with CSL expression were enriched for families related to complement system, proliferation, blood vessel morphogenesis and suppression of apoptosis (via NF- κ B). By contrast, oppositely correlated genes were enriched for families related to cytoskeleton and cell adhesion, mitosis and meiosis, epithelial-to-mesenchymal transition and development, protein folding and DNA damage. Among CSL positively or negatively correlated genes many were transcription factors, as shown in Fig. 1J. For further studies on a possible connection between CSL expression and these various cellular functions, we focused on DNA damage response.

3) Stress / DNA damaging conditions as negative regulators of CSL expression

Intrigued by the possibility that DNA damage as a consequence of stress could regulate CSL levels, we assessed levels of CSL expression in various HDF strains upon exposure to UVA, the form of UV light with higher penetration power, capable of reaching the dermal compartment of the skin and directly affecting dermal fibroblasts.¹⁵ RT-qPCR analysis showed that CSL expression was down-modulated in all tested HDF strains at various times after UVA exposure, with CDKN1A being oppositely regulated (Fig. 2A, B).

UVA is a major cause of skin photoaging and cancer, with production of reactive oxygen species (ROS) as main mediator of its effects, including

those on the DNA.¹⁶ As with UVA, CSL down-modulation and CDKN1A up-regulation were observed upon treatment of several HDF strains with glucose oxidase, which results in continuous production of ROS via oxidation of glucose in gluconolactone and hydrogen peroxide¹⁷ (Fig. 2C). Similar results were observed after treating cells with extracts of cigarette smoke, another potent inducer of oxidative stress – as well as DNA damage¹⁸ (Fig. 2D). Chemotherapeutic DNA-damaging agents have also been reported to cause stromal fibroblasts senescence and CAF activation.¹⁹ As in response to the other insults, treatment with doxorubicin resulted in down-regulation of CSL and opposite CDKN1A induction (Fig. 2E).

4) p53 as a negative regulator of CSL expression.

The opposite regulation of CSL and CDKN1A expression in response to several stress/DNA damaging conditions suggested that p53 may be involved. To directly assess whether p53 functions as a negative regulator of CSL expression, HDFs were stably infected with a lentivirus for inducible p53 expression. As shown in Fig. 3A and B, induction of wild-type p53 resulted in consistent down-regulation of CSL, at both RNA and protein levels, in all tested HDF strains. No such effects were observed after similar expression of a DNA binding domain p53 mutant protein (R248W) (Fig. 3A, B).

As an alternative approach, HDFs were treated with Nutlin-3a, a MDM2 inhibitor and inducer of endogenous p53 activity through p53 protein stabilization. Even in this case, CSL expression was consistently down-regulated in all tested strains (Fig. 3C, D). A detailed time course after Nutlin-

3a treatment showed p53 accumulation and concomitant induction of p21 (as a read-out for p53 activation) preceding CSL down-modulation (Fig. 3E, F).

Mirroring these results, p53 silencing in several strains of HDFs led to a significant induction of CSL expression both at RNA and protein levels (Fig. 3G, H).

5) Multiple mechanisms of negative control of CSL expression by p53

One mechanism whereby p53 can negatively control expression of target genes is through direct weak binding to their regulatory regions.²⁰ The CSL locus encompasses more than 150 kb. Bioinformatic analysis (with MatInspector, Genomatix) of the enhancer and promoter regions (identified on the basis of the human primary fibroblasts data in the ENCODE database) (Fig. 4A) revealed the presence of 144 putative binding sites for p53. To assess whether p53 binds to any of these, we performed ChIP-seq (ChIP combined with massive parallel DNA sequencing) analysis of HDFs under basal conditions and after p53 stabilization by Nutlin-3a treatment (Fig. 4B) (GSE77371). As a positive p53 target, we analyzed the CDKN1A locus and found, as expected, 3 regions of p53 strong binding under basal conditions, with 2 additional binding peaks in Nutlin-3a treated cells (Fig. 4B, upper panel and Supplementary Table 3). By contrast, at the CSL locus, we found a single p53 binding peak, only in the Nutlin-3a treated cells (Fig. 4B, middle panel and Supplementary Table 3). This was located in intron 4 of the CSL gene, a position outside of predicted regulatory regions and consistent with the one found in a previous survey of p53 binding sites in IMR90 lung fibroblasts²¹ (Data accessible at NCBI's GEO database²², accession GSE31558). The

binding peak enrichment for p53 at the CSL locus was lower than those at the CDKN1A locus but comparable to the one we found at the PTK2 (Fak kinase) gene (Fig. 4B, lower panel and Supplementary Table 3), a previously reported gene under direct negative p53 control.^{23, 24}

Despite the lack of ChIP-seq p53 binding peaks in regulatory regions of the CSL locus, weaker p53 binding cannot be ruled out due to the relatively low sensitivity of the method. Sequence analysis of the CSL promoter region (chr4: 26320712–26322647) revealed the presence of three predicted p53 binding sites, two clustered upstream of the transcription start site (BS1 and BS2) and the other in the first intronic region (BS3) (Fig. 4C, top panel). These sites have various mismatches relative to the consensus p53 recognition sequence, which may result in a low binding affinity.^{25, 26} In fact, direct chromatin immunoprecipitation (ChIP) assays showed only weak p53 binding to these sites, in Nutlin-3a treated HDFs, in contrast to the more significant binding to the intron 4 region of the CSL gene or the CDKN1A promoter (Fig. 4C, bottom panel).

Bioinformatic analysis of genomic variations in the human population showed the presence of a single nucleotide polymorphism (SNP; rs7657866) that abrogates the predicted p53 recognition sequence of the BS3 site in the CSL promoter (as determined by MatInspector, Genomatix). The minor nucleotide allele (A) is present in a homozygous form in 8.42% of the human population and in 33,2% in heterozygous form with the major allele (G). In our collection of HDF strains, by direct nucleotide sequencing we found three strains with the A/A genotype. Modulation of endogenous CSL expression in these strains in response to Nutlin 3-a treatment was not consistently different

from that of strains harboring the major allele. To directly assess whether p53 can negatively control CSL promoter activity and whether in this context the identified SNP is of functional significance, we cloned the CSL promoter spanning this region from cells homozygous for both the G/G and A/A alleles. As shown in Fig. 4D, activity of the CSL promoter with the major G/G allele (CSLpr-1.94kb G/G) was effectively suppressed by p53 in a dose-dependent manner. Activity of the CSL promoter with the minor A/A allele was differentially suppressed by p53, requiring higher concentrations (Fig. 4D).

Besides direct binding to negative target genes, another complementary mechanism by which p53 can negatively control gene expression is through one of its effectors, CDKN1A (p21).²⁷ To assess whether increased p21 levels reproduce the effects of p53 activation on CSL gene transcription, HDFs were infected with a lentivirus expressing p21. As shown in Fig.4E and F, increased p21 levels resulted in suppression of CSL expression, similarly to what we observed after induction of p53 expression.

Discussion

Gene expression can vary significantly between individuals, possibly accounting for different susceptibility to complex trait diseases like cancer.²⁸ CSL functions in stromal fibroblasts as direct repressor of senescence and CAF-determinant genes, and down-modulation of CSL expression is a key step for CAF conversion.⁴ An important question is therefore how this gene is controlled. CSL is best known for its role as key effector of canonical Notch signaling. However, the negative correlation between CSL and Notch1

expression in primary fibroblasts derived from a large number of individuals suggests that the two genes play a separate and possibly opposite function in these cells. Gene ontology analysis revealed that among gene families negatively correlated with CSL expression several were involved in cytoskeleton rearrangements, known to be a feature of myofibroblasts and CAF activation.^{29, 30} On the other hand, the top positively correlated genes were involved in the complement system, with a predominance of RCA/CCP (regulators of complement activation/ complement control proteins) genes, such as Factor H, C1 inhibitor and MCP. The role of the complement system in cancer has long been debated³¹: on one hand, complement is thought to be supportive of the immune-mediated killing of tumor cells. On the other hand, complement activation promotes inflammation, which is correlated with tumor onset and progression.³² The “complement” genes that we found to be positively correlated with CSL are negative regulators of complement activation. This arises the exciting possibility that an important element of CAF conversion resulting from compromised CSL is complement activation, which provides an inflammatory tumor-inducing environment.³³ Variations in CSL expression levels correlated significantly also with a large number of genes that may be both downstream CSL targets and/or upstream regulators. Among the first category are likely genes involved in CAF determination, coding for a number of growth factors / cytokines as well as determinants of cytoskeleton organization and cell motility. Among the second category of genes are likely those involved in the DNA damage/stress response.

A number of exogenous insults leading to direct or indirect DNA damage, such as UVA irradiation, exposure to Reactive Oxygen Species

(ROS), smoke extracts and doxorubicin, caused down-modulation of CSL expression in the tested fibroblast strains. UVA is thought to be an important etiological factor of skin photo-aging and cancer^{15, 34} and, due to its great penetration power, it can directly affect the dermal compartment of the skin. Its effects are mostly mediated by the enhanced production of Reactive Oxygen Species (ROS), which cause secondary DNA damage as well as changes in many other aspects of cell physiology.³⁵ Cigarette smoke extract, another stress inducer, is composed by several toxic compounds, such as nicotine and hydrogen monoxide, which target directly or indirectly the DNA and induce fibroblast senescence and CAF activation.¹⁸ Doxorubicin, a chemotherapeutic DNA damaging agent, also causes stromal fibroblast senescence and CAF activation.¹⁹ All these stress conditions resulted in significant down-modulation of CSL expression with concomitant induction of CDKN1A levels, a common indicator of p53 activity. While we focused on p53 for further studies, UVA exposure represses CSL expression also in HDFs with p53 gene silencing (Supplementary Fig. 1A, B), indicating that other determinants of the DNA damage / stress response converge on negative regulation of this gene. A possible mechanism is promoter DNA methylation, as CSL expression is down-modulated with the same kinetics of Notch2 (Supplementary Fig. 1C), whose down-modulation upon UVA treatment is due to DNA methylation.²

The transcriptional repressing function of p53 is relatively poorly understood.³⁶ It can be mediated, in part, by direct p53 binding to target genes. It has been proposed that the p53 consensus recognition sequences of induced and repressed genes are different, with validated repressor sites

having a weaker affinity with longer spacers between quarter-sites and/or changed orientation of these sites.²⁶ We identified a specific site within the CSL locus in intron 4, to which p53, at enhanced levels, binds. However, this site has a complete p53 responsive element with a theoretical high transactivation score and lies outside any predicted regulatory regions of the CSL gene, making it unlikely to be involved in negative control of its expression. More functionally relevant is likely to be the ability of p53 to negatively control CSL promoter activity. Indeed we show that CSL promoter activity is suppressed in exogenous assays by increased p53 in a dose dependent manner, with lesser inhibition resulting from a nucleotide polymorphism in the CSL promoter abrogating a p53 recognition sequence.

Another mechanism by which p53 can negatively control gene transcription is through one or more of its effectors, such as p21 (CDKN1A). p21 can function as a negative regulator of gene expression, independently of its effects on the cell cycle, through a variety of mechanisms including binding and negative regulation of E2F1 activity^{27, 37-39}, recruitment of E2F4 repression complexes³⁷, and binding and modulation of Estrogen Receptor alpha –dependent transcription.⁴⁰ The impact of increased or decreased p21 activity in stromal fibroblasts remains to be conclusively established, as it has been variously reported that p21 overexpression induces CAF conversion⁴¹ or only cellular senescence without induction of the senescence-associated CAF-related secretory phenotype.⁴² In our own work, we found that silencing of the p21 gene, like that of p53, can synergize with CSL knockdown in induction of CAF marker expression⁴, pointing to an overlap of p53 and p21 transcription repressive function beyond control of the CSL gene.

Overall, an emerging scenario exists of a reciprocal negative feedback loop between p53 and CSL activity, which could be responsible for overriding individual differences in gene expression, allowing a proper response to stress factors and thus maintaining stromal tissue homeostasis. We recently showed that CSL directly binds to p53 suppressing its activity and, as part of the chronic process leading to cancer development, p53-induced senescence can function as fail-safe mechanism against cancer/stromal cell expansion resulting from compromised CSL function.⁴ In turn, the present findings indicate that p53 negatively controls CSL expression, thus providing a positive feedback mechanism for enforcement of p53 activity in the acute response of cells to DNA damaging cancer-threatening conditions (Fig. 4G).

Materials and methods

Human samples and cell culture

Discarded human foreskin tissue samples for primary cell preparation were obtained from the Department of Pediatrics, Lausanne University Hospital, with institutional approvals and informed consent as part of institutional requirements.

Conditions for culturing of cells, viral infection, siRNA-mediated gene silencing, RT-qPCR and ChIP were as previously reported.^{2, 43, 44} For derivation of HDFs, surgically excised foreskins were fragmented into pieces after removal of the hypodermis, followed by incubation in 1% collagenase I solution at 37°C under shaking. The dissociated tissue was diluted, filtered and washed by centrifugation and subsequently cultured in 10% FBS DMEM without Phenol Red (Gibco), in order to avoid any absorbance of UV light by

the medium. For stress inducing experiments, cells were treated when they reached 60% confluence. UVA irradiation ($1\text{J}/\text{cm}^2$) was performed in a UVA irradiator (Vilber) monitored with a dosimeter (InternationalLight.Inc). Chemicals used for the study were as follows: 20 mU/ml of glucose oxidase (Sigma), 50 $\mu\text{g}/\text{ml}$ of Cigarette Smoke Extract (Murty Pharmaceuticals), 0.4 μM of doxorubicin hydrochloride (Sigma), 10 μM of Nutlin-3a (Sigma) or suitable controls. Doxycycline hyclate (Sigma) was used at a dose of 750 ng/ml at the indicated time in experiments with cells transduced with lentiviruses for doxycycline-inducible expression.

RT-qPCR and immunoblotting

RT-qPCR were carried out as previously described ⁴ in triplicate using the following primers: 36 β 4 Fwd: 5'-GCAATGTTGCCAGTGTCTGT-3', Rev: 5'-GCCTTGACCTTTTCAGCAAG-3'; CSL Fwd: 5'-GGCTGGAATACAAGTTGAACA-3', Rev: 5'-AGAGCAAAAGCTCAAAGGTG-3'; p21 Fwd: 5'-AGCAGAGGAAGACCATGTGGACCT-3', Rev: 5'-GAAGATGTAGAGCGGGCCTTTGAGG-3'. Immunoblotting experiments were carried out as previously described ⁴ using the following antibodies: for CSL, D10A4 (Cell Signaling), for p53, sc-126 (Santa Cruz Biotechnology) and for γ -tubulin, clone GTU-88 (Sigma). 20 μg of proteins were loaded on 10% acrylamide gels, and detection was performed using the infrared fluorescent IRDye® secondary antibodies (LI-COR®) and the Odyssey CLx (LI-COR®) infrared imaging system. Image analysis were performed using the Image Studio software (LICOR®).

Plasmids and siRNAs

To make the pIND20-p53WT and pIND20-p53R248W plasmids, PCR products using the primers Fwd: 5'-CACCATGGAGGAGCCGCGAGTCAGATCCTAGCGTCGA-3' and Rev: 5'-TCAGTCTGAGTCAGGCCCTTCTGTCTTGAA-3' and pBABE-puro-p53WT and pBABE-puro-p53R248W vectors as respective templates (obtained from Dr A. Rustgi, University of Pennsylvania, PA ⁴⁵), were cloned into the pENTR-D-TOPO entry vector (Life Technologies) and transferred through the Gateway LR Clonase system (Life Technologies) into the pINDUCER20 destination vector ⁴⁶ using the pENTRTM directional TOPO cloning kit. The same strategy was used to produce pIND20-CSL, using the following PCR primers Fwd: 5'-CACCATGGACCACACGGAGGGCTCGCCCGCGGAGGAGCC-3' and Rev: 5'-TTAGGATAACCACTGTGGCTGTAGATGATGTGAC-3'. with pBMNRBPj plasmid ⁴⁷ as template. The pIND20-p21 was obtained from Dr SJ Elledge (Brigham and Women's Hospital, Boston, MA) ⁴⁶. The pRS-p53 (shp53) and control pRS vectors were obtained from Dr. R. Agami (The Netherlands Cancer Institute, Amsterdam, The Netherlands).

RNAseq analysis

Total RNAs from HDFs were extracted using the directZol RNA miniprep kit (Zymo Research) with on-column DNase treatment. RNA quality was verified on the Bioanalyzer (Agilent) and 1 µg of total RNA with RIN > 8 was used for library preparation using the NEBNext® Ultra kit (NEB) according to manufacturer instructions. Single read was done on the Illumina HiSeq 2000

sequencer at the Genomic Technologies Facility (University of Lausanne). Sequencing quality check was performed using FastQC (v 0.10.1 <http://www.bioinformatics.babraham.ac.uk/projects/fastqc/>). PolyA tails, adapter sequences and low quality reads were cut using Cutadapt⁴⁸ (v 1.4.1), using a base quality cutoff of 5. The alignment was performed using Tophat2⁴⁹ (v 2.0.9) and GRCh37 as reference genome. Reads were sorted by position in the reference genome using Picard (<http://broadinstitute.github.io/picard/> v 1.96). Indexing was performed using sambamba (<http://lomerreiter.github.io/sambamba/> v 0.4.7) and alignment statistics using bamtool stats (<http://sourceforge.net/projects/bamtools/> v 2.3.0). RNAseq quality was checked using the R package NOISeq⁵⁰ (v 2.6.0), analyzing coverage, percentage of reads mapping to different genes and fraction of rRNA. Reads were counted and gene expression evaluated using HTSeq (v 0.6.1).

Data have been deposited in NCBI's Gene Expression Omnibus²² and are accessible through GEO series accession number GSE77370 (<http://www.ncbi.nlm.nih.gov/geo/query/acc.cgi?acc=GSE77370>).

Bioinformatic analyses

The graphic illustrations showing the correlation analysis between various genes and CSL were produced using the R package corrplots (v 0.73), starting from the RNAseq RPKM reads. Correlation analyses were performed on the matrix of log₂ RPKM values for the 46 foreskin samples after combat algorithm to adjust data for batch effect⁵¹. Genes with $|\text{Pearson coefficient}| > 0.5$ and $p < 0.0005$ were considered as significantly correlated to CSL.

Correlation matrices were generated in R using the cor() function. The corrplot package was then used to graphically display correlation matrices. The functional annotation tool available within DAVID Website (<http://david.abcc.ncifcrf.gov/>) was used to look for any over-represented biological process level 5 (BP5) of the Gene Ontology (GO). Process networks and pathway maps analysis was performed with MetaCore™ version 6.2 (Thomson Reuters).

Locus analysis, ChIP assay and ChIP-seq

For human CSL locus analysis, we used ENCODE data (<http://genome.ucsc.edu/ENCODE>) giving information on chromatin organization. Based on the Chromatin in State Segmentation by HMM data, we defined promoters and enhancers in the CSL locus. Exons were defined taking in account all exons described for the four main CSL transcript variants described in the NCBI database. The variants analyzed are: NM_005349.3, NM_203283.2, NM_015874.4, NM_203284.2.

ChIP assays with antibodies against p53 versus non-immune IgG control were carried out as previously described ⁴ followed by determination of binding enrichment for the indicated sites; primer sequences were as follows:

CDKN1Apr_BSF: 5'-TGGACTGGGCACTCTTGTC-3',	CDKN1Apr_BSR: 5'-
AGAAAGCCAATCAGAGCCAC-3',	negativeCTRL_BSF: 5'-
CCCTAATGGTCTAAAAGGG-3',	negativeCTRL_BSR: 5'-
ACTACCACTTACAGTGCCTG-3',	CSLintron4_BSF: 5'-
TTTCCAATAAGGAAGGGGC-3',	CSLintron4_BSR: 5'-

CTCTAAAGCCTCCTATCAAC-3'.	CSLpr_BS1.2F:	5'-
GGCGCCCGGAGCTGGT-3'	CSLpr_BS1.2R:	5'-
TGGGAAATTTCTAAACCTCG-3'	CSLpr_BS3F:	5'-
AAGGGCCTCCTCATTAGCAT-3'	CSLpr_BS3R:	5'-

TAATCTCGGCGTTTGGTGCA-3'. CDKN1Apr_BS primers were used as a

positive control for binding of p53 to the CDKN1A promoter. negativeCTRL_BS were primers designed for a putative p53 binding site in the enhancer of CSL, which was not confirmed, and were used as a negative control for p53 binding.

For ChIP-seq analysis, immunoprecipitated DNA from HDFs was processed as for ChIP assays ⁴ using 5 µg of antibody against p53 per 10⁶ cells. The ChIPed DNA was quantified by fluorimetry on a Qubit system (Invitrogen). A total of 10 ng of DNA was used for library preparation using a NEBNext ChIP-Seq Library Prep reagent set (New England Biolabs Inc.), as recommended by the manufacturer. The sequencing was performed by the Genomic Technologies Facility at Lausanne University. Sequencing quality control was performed using FASTqc ⁵²; immunoprecipitation quality control was performed using PhantomPeak ⁵³ quality tools and CHANCE ⁵⁴. Burrows–Wheeler Aligner ⁵⁵ was used for FASTQ file alignments and, for peak detection, MACS software ⁵⁶ with default parameters was used. Each peak was associated to the closest transcription starting sites with ChIPpeakAnno ⁵⁷, a Bioconductor R package. The Integrative Genomics Viewer (IGV) (<http://www.broadinstitute.org/igv>) was used for graphic illustration of ChIP-Seq peaks, and ENCODE data (<http://genome.ucsc.edu/ENCODE>) for information on chromatin organization. ChIP-Seq data have been deposited in

NCBI's Gene Expression Omnibus ²² and are accessible through GEO series accession number GSE77225 (<http://www.ncbi.nlm.nih.gov/geo/query/acc.cgi?acc=GSE77225>).

For SNP analysis, the 1000 genome database was used in the SPSmart program (<http://spsmart.cesga.es>).

Promoter activity assay

The CSL promoter-1.94 kb vector (CSLpr-1.94kb) (chr4: 26,320,712–26,322,647) was obtained by amplification of the PCR product using the following primers Fwd- 5'AGACTAGGTGACTCAAGGCA-3' and Rev- 5'-CCACAAACTCTCGCCAAAAC-3' and human genomic DNA as template. The PCR fragment was inserted into the pGL3-enhancer vector (Promega, Firefly luciferase) in the BglII/XhoI site and sequence was verified by DNA sequencing. HDFs were co-transfected in triplicate with the CSLpr-1.94kb (0.5 µg/well) together with the indicated amounts of pBABE-p53WT plasmid (obtained from Dr A. Rustgi (University of Pennsylvania, PA)⁴⁵) as well as 0.05 ug of the phRL-TK plasmid (Promega, Renilla luciferase for internal control). Luciferase activity was determined with the Dual Luciferase assay kit (Promega) 30 hours later, using internal Renilla control for normalization.

Statistical analysis

Two-tailed Student's *t*-tests were performed where appropriate unless specified. Error bars represent SD. P values are as indicated in figure legends.

Supplementary Materials

Supplementary Table 1. RPKM values from RNAseq analysis for each HDF strain.

Supplementary Table 2. List of genes whose expression is positively or negatively correlated to CSL plus gene ontology analyses as determined in Figure 1 (related to Figure 1I and J).

Supplementary Table 3. Genomic coordinates of p53 binding peaks in CSL, CDKN1A and PTK genes, as revealed by ChIP-seq analysis in HDFs (related to Figure 4A-C).

Supplementary Figure 1. P53 is not the main effector of UVA-induced CSL down-regulation.

Acknowledgments

We thank R. Bernards, R. Agami, A. Rustgi and SJ Elledge for the gift of various viral vectors, K. Harshman, P. Angelino and V. Ioannidis for RNA-seq, ChIP-seq DNA sequencing analysis and bioinformatic support. We are grateful to Corentin Pasche and Tatiana Proust for technical help. This work was supported by grants from the Swiss National Science Foundation (310030_156191/1), the National Institute of Arthritis and Musculoskeletal and Skin Diseases (R01AR039190; R01AR064786; the content not necessarily representing the official views of NIH), European Research Council (26075083) and Swiss Cancer League (OCS-2922-02-2012 and KFS-3301-08-2013). E. Menietti was supported by a grant from ISREC and P. Ostano by a grant from Lauretana S .P.A.

References

1. Johnson JE, Macdonald RJ. Notch-independent functions of CSL. *Curr Top Dev Biol* 2011; 97:55-74.
2. Hu B, Castillo E, Harewood L, Ostano P, Reymond A, Dummer R, Raffoul W, Hoetzenecker W, Hofbauer GF, Dotto GP. Multifocal epithelial tumors and field cancerization from loss of mesenchymal CSL signaling. *Cell* 2012; 149:1207-20.
3. Dotto GP. Multifocal epithelial tumors and field cancerization: stroma as a primary determinant. *J Clin Invest* 2014; 124:1446-53.
4. Procopio MG, Laszlo C, Al Labban D, Kim DE, Bordignon P, Jo SH, Goruppi S, Menietti E, Ostano P, Ala U, et al. Combined CSL and p53 downregulation promotes cancer-associated fibroblast activation. *Nature cell biology* 2015; 17:1193-204.
5. Bray SJ. Notch signalling: a simple pathway becomes complex. *Nature reviews Molecular cell biology* 2006; 7:678-89.
6. Liu F, Posakony JW. An enhancer composed of interlocking submodules controls transcriptional autoregulation of suppressor of hairless. *Dev Cell* 2014; 29:88-101.
7. Choi VN, Park SK, Hwang BJ. Clustered LAG-1 binding sites in lag-1/CSL are involved in regulating lag-1 expression during lin-12/Notch-dependent cell-fate specification. *BMB Rep* 2013; 46:219-24.
8. Collu GM, Hidalgo-Sastre A, Acar A, Bayston L, Gildea C, Leverentz MK, Mills CG, Owens TW, Meurette O, Dorey K, et al. Dishevelled limits Notch signalling through inhibition of CSL. *Development* 2012; 139:4405-15.
9. Kim SM, Kim MY, Ann EJ, Mo JS, Yoon JH, Park HS. Presenilin-2 regulates the degradation of RBP-Jk protein through p38 mitogen-activated protein kinase. *J Cell Sci* 2012; 125:1296-308.
10. Wacker SA, Alvarado C, von Wichert G, Knippschild U, Wiedenmann J, Clauss K, Nienhaus GU, Hameister H, Baumann B, Borggreffe T, et al. RITA, a novel modulator of Notch signalling, acts via nuclear export of RBP-J. *EMBO J* 2011; 30:43-56.

11. Zhou S, Hayward SD. Nuclear localization of CBF1 is regulated by interactions with the SMRT corepressor complex. *Mol Cell Biol* 2001; 21:6222-32.
12. Consortium GT. Human genomics. The Genotype-Tissue Expression (GTEx) pilot analysis: multitissue gene regulation in humans. *Science* 2015; 348:648-60.
13. Dotto GP. Crosstalk of Notch with p53 and p63 in cancer growth control. *Nat Rev Cancer* 2009; 9:587-95.
14. Kopan R. Notch signaling. *Cold Spring Harbor perspectives in biology* 2012; 4.
15. Halliday GM. Inflammation, gene mutation and photoimmunosuppression in response to UVR-induced oxidative damage contributes to photocarcinogenesis. *Mutat Res* 2005; 571:107-20.
16. Bachelor MA, Bowden GT. UVA-mediated activation of signaling pathways involved in skin tumor promotion and progression. *Seminars in cancer biology* 2004; 14:131-8.
17. Wong CM, Wong KH, Chen XD. Glucose oxidase: natural occurrence, function, properties and industrial applications. *Appl Microbiol Biotechnol* 2008; 78:927-38.
18. Laytragoon-Lewin N, Bahram F, Rutqvist LE, Turesson I, Lewin F. Direct effects of pure nicotine, cigarette smoke extract, Swedish-type smokeless tobacco (Snus) extract and ethanol on human normal endothelial cells and fibroblasts. *Anticancer research* 2011; 31:1527-34.
19. Soon PS, Kim E, Pon CK, Gill AJ, Moore K, Spillane AJ, Benn DE, Baxter RC. Breast cancer-associated fibroblasts induce epithelial-to-mesenchymal transition in breast cancer cells. *Endocrine-related cancer* 2013; 20:1-12.
20. Chen X, Wang J, Shen H, Lu J, Li C, Hu DN, Dong XD, Yan D, Tu L. Epigenetics, microRNAs, and carcinogenesis: functional role of microRNA-137 in uveal melanoma. *Investigative ophthalmology & visual science* 2011; 52:1193-9.
21. Botcheva K, McCorkle SR, McCombie WR, Dunn JJ, Anderson CW. Distinct p53 genomic binding patterns in normal and cancer-derived human cells. *Cell cycle* 2011; 10:4237-49.

22. Edgar R, Domrachev M, Lash AE. Gene Expression Omnibus: NCBI gene expression and hybridization array data repository. *Nucleic Acids Res* 2002; 30:207-10.
23. Golubovskaya VM, Finch R, Kweh F, Massoll NA, Campbell-Thompson M, Wallace MR, Cance WG. p53 regulates FAK expression in human tumor cells. *Molecular carcinogenesis* 2008; 47:373-82.
24. Golubovskaya V, Kaur A, Cance W. Cloning and characterization of the promoter region of human focal adhesion kinase gene: nuclear factor kappa B and p53 binding sites. *Biochimica et biophysica acta* 2004; 1678:111-25.
25. Menendez D, Inga A, Resnick MA. The expanding universe of p53 targets. *Nature reviews Cancer* 2009; 9:724-37.
26. Riley T, Sontag E, Chen P, Levine A. Transcriptional control of human p53-regulated genes. *Nature reviews Molecular cell biology* 2008; 9:402-12.
27. Lohr K, Moritz C, Contente A, Dobbelstein M. p21/CDKN1A mediates negative regulation of transcription by p53. *J Biol Chem* 2003; 278:32507-16.
28. Barbujani G, Colonna V. Human genome diversity: frequently asked questions. *Trends Genet* 2010; 26:285-95.
29. Kalluri R, Zeisberg M. Fibroblasts in cancer. *Nature reviews Cancer* 2006; 6:392-401.
30. Tomasek JJ, Gabbiani G, Hinz B, Chaponnier C, Brown RA. Myofibroblasts and mechano-regulation of connective tissue remodelling. *Nature reviews Molecular cell biology* 2002; 3:349-63.
31. Markiewski MM, Lambris JD. Is complement good or bad for cancer patients? A new perspective on an old dilemma. *Trends in immunology* 2009; 30:286-92.
32. Pio R, Ajona D, Lambris JD. Complement inhibition in cancer therapy. *Seminars in immunology* 2013; 25:54-64.
33. Merle NS, Noe R, Halbwachs-Mecarelli L, Fremeaux-Bacchi V, Roumenina LT. Complement System Part II: Role in Immunity. *Frontiers in immunology* 2015; 6:257.
34. Rittie L, Fisher GJ. UV-light-induced signal cascades and skin aging. *Ageing research reviews* 2002; 1:705-20.

35. Kawanishi S, Hiraku Y, Oikawa S. Mechanism of guanine-specific DNA damage by oxidative stress and its role in carcinogenesis and aging. *Mutat Res* 2001; 488:65-76.
36. Wang B, Xiao Z, Ko HL, Ren EC. The p53 response element and transcriptional repression. *Cell cycle* 2010; 9:870-9.
37. Benson EK, Mungamuri SK, Attie O, Kracikova M, Sachidanandam R, Manfredi JJ, Aaronson SA. p53-dependent gene repression through p21 is mediated by recruitment of E2F4 repression complexes. *Oncogene* 2014; 33:3959-69.
38. Devgan V, Mammucari C, Millar SE, Brisken C, Dotto GP. p21WAF1/Cip1 is a negative transcriptional regulator of Wnt4 expression downstream of Notch1 activation. *Genes & development* 2005; 19:1485-95.
39. Delavaine L, La Thangue NB. Control of E2F activity by p21Waf1/Cip1. *Oncogene* 1999; 18:5381-92.
40. Fritah A, Saucier C, Mester J, Redeuilh G, Sabbah M. p21WAF1/CIP1 selectively controls the transcriptional activity of estrogen receptor alpha. *Mol Cell Biol* 2005; 25:2419-30.
41. Capparelli C, Chiavarina B, Whitaker-Menezes D, Pestell TG, Pestell RG, Hult J, Ando S, Howell A, Martinez-Outschoorn UE, Sotgia F, et al. CDK inhibitors (p16/p19/p21) induce senescence and autophagy in cancer-associated fibroblasts, "fueling" tumor growth via paracrine interactions, without an increase in neo-angiogenesis. *Cell cycle* 2012; 11:3599-610.
42. Freund A, Patil CK, Campisi J. p38MAPK is a novel DNA damage response-independent regulator of the senescence-associated secretory phenotype. *EMBO J* 2011; 30:1536-48.
43. Hu B, Lefort K, Qiu W, Nguyen BC, Rajaram RD, Castillo E, He F, Chen Y, Angel P, Brisken C, et al. Control of hair follicle cell fate by underlying mesenchyme through a CSL-Wnt5a-FoxN1 regulatory axis. *Genes & development* 2010; 24:1519-32.
44. Lefort K, Mandinova A, Ostano P, Kolev V, Calpini V, Kolfshoten I, Devgan V, Lieb J, Raffoul W, Hohl D, et al. Notch1 is a p53 target gene involved in human keratinocyte tumor suppression through negative regulation of ROCK1/2 and MRCKalpha kinases. *Genes & development* 2007; 21:562-77.

45. Okawa T, Michaylira CZ, Kalabis J, Stairs DB, Nakagawa H, Andl CD, Johnstone CN, Klein-Szanto AJ, El-Deiry WS, Cukierman E, et al. The functional interplay between EGFR overexpression, hTERT activation, and p53 mutation in esophageal epithelial cells with activation of stromal fibroblasts induces tumor development, invasion, and differentiation. *Genes & development* 2007; 21:2788-803.
46. Meerbrey KL, Hu GA, Kessler JD, Roarty K, Li MZ, Fang JE, Herschkowitz JI, Burrows AE, Ciccio A, Sun TT, et al. The pINDUCER lentiviral toolkit for inducible RNA interference in vitro and in vivo. *P Natl Acad Sci USA* 2011; 108:3665-70.
47. Liang Y, Ganem D. Lytic but not latent infection by Kaposi's sarcoma-associated herpesvirus requires host CSL protein, the mediator of Notch signaling. *Proc Natl Acad Sci U S A* 2003; 100:8490-5.
48. MARTIN M. Cutadapt removes adapter sequences from high-throughput sequencing reads. *EMBnetjournal* 2011; 17:10-2.
49. Langmead B, Trapnell C, Pop M, Salzberg SL. Ultrafast and memory-efficient alignment of short DNA sequences to the human genome. *Genome biology* 2009; 10:R25.
50. Tarazona S, Garcia-Alcalde F, Dopazo J, Ferrer A, Conesa A. Differential expression in RNA-seq: a matter of depth. *Genome Res* 2011; 21:2213-23.
51. Johnson WE, Li C, Rabinovic A. Adjusting batch effects in microarray expression data using empirical Bayes methods. *Biostatistics* 2007; 8:118-27.
52. Patel RK, Jain M. NGS QC Toolkit: a toolkit for quality control of next generation sequencing data. *Plos One* 2012; 7:e30619.
53. Jung LY KP, Wold B, Sidow A, Batzoglou S, Park P. Assessment of ChIP-seq data quality using cross-correlation analysis. (Submitted).
54. Diaz A, Nellore A, Song JS. CHANCE: comprehensive software for quality control and validation of ChIP-seq data. *Genome biology* 2012; 13:R98.
55. Li H, Durbin R. Fast and accurate short read alignment with Burrows-Wheeler transform. *Bioinformatics* 2009; 25:1754-60.

56. Zhang Y, Liu T, Meyer CA, Eeckhoute J, Johnson DS, Bernstein BE, Nusbaum C, Myers RM, Brown M, Li W, et al. Model-based analysis of ChIP-Seq (MACS). *Genome biology* 2008; 9:R137.

57. Zhu LJ, Gazin C, Lawson ND, Pages H, Lin SM, Lapointe DS, Green MR. CHIPpeakAnno: a Bioconductor package to annotate ChIP-seq and ChIP-chip data. *BMC bioinformatics* 2010; 11:237.

Figure legends

Fig. 1. Individual variations in gene expression in HDFs. (A-D) Second passage HDFs from 48 different individuals were analyzed by RNA sequencing. Shown are RPKM (reads per kilobase transcriptome per million mapped reads) values for the indicated genes (See also Supplementary Table 1). **(E)** Comparison of DLL1 RNA expression levels obtained by RNA sequencing versus RT-qPCR analysis. **(F)** Graphic illustrations of Pearson's R correlation analysis carried out on log₂ RPKM values from RNAseq data used in A-D, for indicated Notch signaling pathway components against each other or against CSL. Blue and red squares correspond to positive and negative values respectively. Significant correlation ($|\text{Pearson score}| > 0.5$) is indicated in the colorimetric scale as green stars. **(G)** Comparative correlation analysis as performed in F between CSL and Notch signaling genes was determined from either RNA-seq or RT-qPCR data. **(H)** Same analysis as in F was performed between CAF markers genes (selected from a previously published list⁴) against each other and against CSL. **(I)** The global set of RNA-seq data used in A-D was analyzed for positive (in blue) or negative (in red) correlation to CSL ($|\text{Pearson score}| > 0.5$, $p < 0.0005$). The list of genes in each group is given in Supplementary Table 2. Gene ontology (Metacore Networks) analysis

with statistically significant enrichment ($p < 0.05$) was performed on genes whose expression is positively (left panel) or negatively (right panel) correlated to CSL levels. **(J)** Shown are genes encoding proteins with transcription factor activity positively (blue) or negatively (red) correlated to CSL selected from Supplementary Table 2.

Fig. 2. Genotoxic and oxidative stresses negatively regulate CSL expression in HDFs. **(A-B)** Indicated strains of HDFs were irradiated with $1\text{J}/\text{cm}^2$ UVA, collected at the indicated time points and CSL (A) and CDKN1A (B) mRNA levels were measured by RT-qPCR using $36\beta 4$ for normalization. $N= 5$ different experiments for Fb79 and 2 for all other strains. **(C)** Indicated strains of HDFs were treated with 20 mU/ml glucose oxidase for 4 hours, and CSL and CDKN1A mRNA levels were measured by RT-qPCR as in A. $N= 2$ different experiments for each strain. **(D)** HDFs (strain Fb79) were treated with 50 $\mu\text{g}/\text{ml}$ of Cigarette Smoke Extract for 48 hours and assessed as in A for CSL and CDKN1A mRNA levels. $N= 2$ different experiments. **(E)** HDFs (strain Fb79) were treated with doxorubicin (0.4 μM) for 24 hours and assessed as in A for CSL and CDKN1A mRNA levels. $N= 2$ different experiments. * $p < 0.0001$, ** $p = 0.0008$.

Fig. 3. p53 is a negative regulator of CSL expression. **(A)** HDFs stably infected with lentiviruses for doxycycline-inducible expression of either wild-type p53 (WTp53) or a R248W mutant p53 (mutp53) versus empty vector (CTRL) were treated with doxycycline (Dox) for 48 hours. CSL mRNA levels were measured by RT-qPCR using $36\beta 4$ for normalization. $N=2$ different

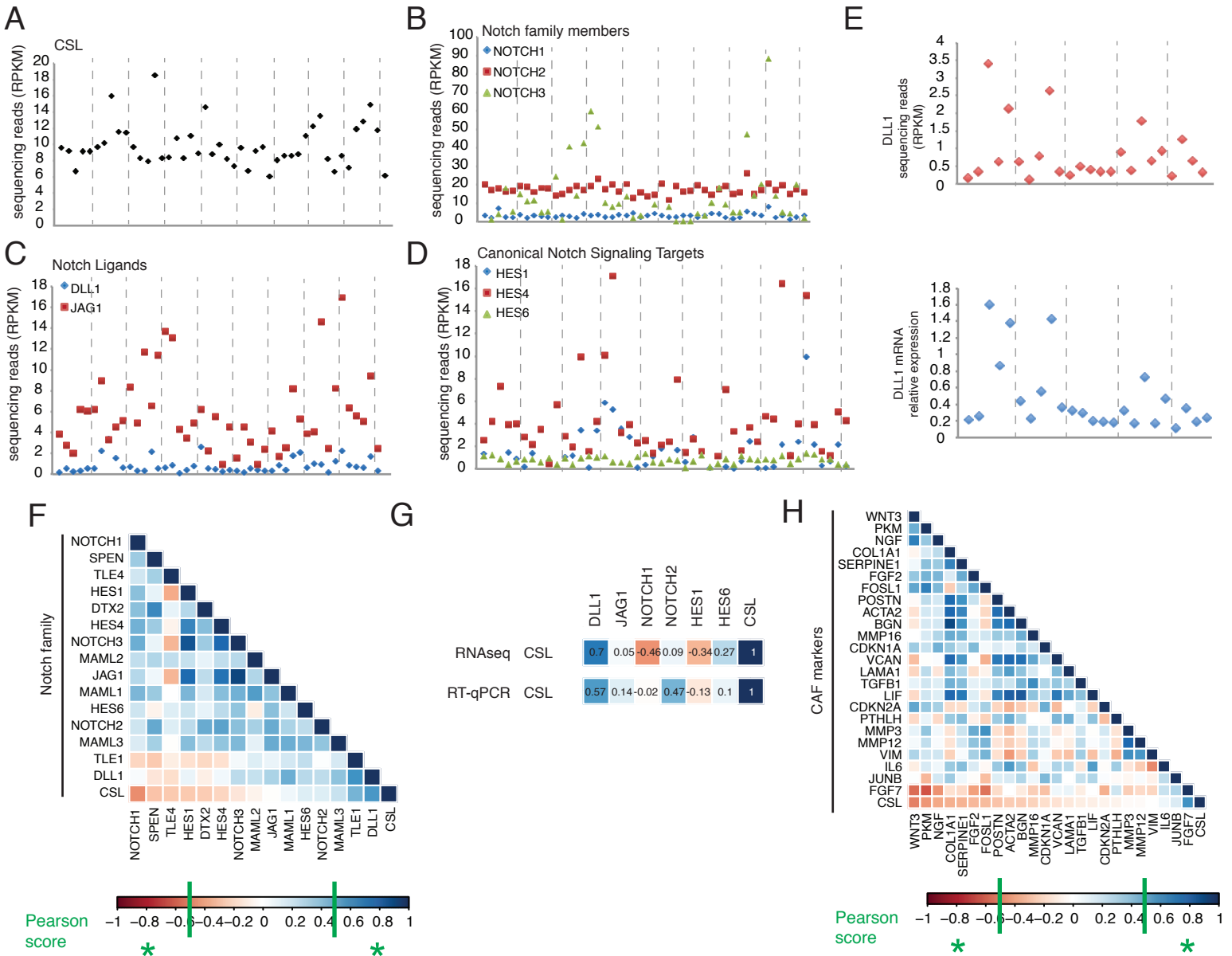
experiments for each strain. **(B)** Indicated HDF strains were treated as in A, and CSL and p53 protein levels were assessed by immunoblot analysis using γ -tubulin as equal loading control. P53, CSL and γ -tubulin blots were performed by sequential blotting of the same membrane without stripping (left panel). Relative protein levels were quantified using the ImageStudio program, with γ -tubulin for normalization (right panel). N=2 different experiments for each strain. **(C and D)** Indicated HDF strains were treated with Nutlin-3a (10 μ M) or DMSO vehicle alone for 48 hours. CSL mRNA (C) and CSL and p53 protein (D) levels were assessed as in A and B, respectively. N=2 different experiments for each strain. **(E and F)** HDFs were treated with Nutlin-3a (10 μ M) or DMSO vehicle for the indicated time points. CSL and p53 protein (E) and p21 mRNA (F) levels were assessed as in B and A, respectively. **(G and H)** Indicated strains of HDFs infected with control (CTRL) versus p53 silencing (shp53) retroviruses were analyzed for CSL mRNA and protein levels as in A and B respectively. N=2 for Fb79 and Fb80. * $p < 0.0001$, ** $p=0.0003$.

Fig. 4. p53 controls CSL expression via multiple mechanisms. (A) Map of the entire CSL locus showing the transcribed region (green bar), transcription start sites (TSS1 and 2) and exons (E1-E11) and, below, localization of insulators (blue), promoters (red) and enhancers (yellow) as predicted for human primary fibroblasts on the basis of the ENCODE data base (as detailed in Materials and Methods). **(B)** Graphic illustrations of ChIP-seq analysis of p53-binding peaks in the CDKN1A, CSL, and PTK2 loci in HDFs treated with Nutlin-3a (10 μ M for 48 hours) or DMSO control (magenta and

blue colors, respectively). P53 binding peaks induced by Nutlin-3a treatment are highlighted (red boxes). A full list of p53-binding peaks is provided in Supplementary Table 2. **(C)** Top: Map of the 1.94 kb CSL promoter region with predicted p53 recognition sequences (blue boxes) and corresponding primers used for the ChIP experiments (magenta arrows) and adjacent exons (green boxes). Bottom: ChIP assay of p53 binding to the CSL promoter and the CSL exon 4 region in HDFs treated for 48 hours with Nutlin-3a (10 μ M) or DMSO control. Binding enrichment to a upstream CSL region devoid of p53 recognition sequences was used as negative control (negative CTRL), while binding to a p53 binding site in the CDKN1A promoter (chr6: 36,644,111-36,644,216) was used as positive control. **(D)** HDFs were co-transfected in triplicate wells with a luciferase reporter construct with the CSL promoter (CSLpr-1.94kb) region shown in the map in (C), with either the G/G or the A/A alleles for the rs7657866 SNP, together with increasing amounts of a plasmid over-expressing p53. Luciferase activity was measured 30 h later, using Renilla internal control for normalization. Shown are results of 2 independent experiments (Exp. 1 and 2). **(E)** HDFs (Fb79) stably infected with lentiviruses for doxycycline-inducible p21 expression were treated or not with doxycycline for 48 hours and CSL mRNA levels measured by RT-qPCR using 36 β 4 for normalization. N=3 independent experiments. **(F)** HDFs (Fb79) were used for immunoblotting with CSL and p53 antibodies using γ -tubulin as equal loading control. CSL and γ -tubulin blots were performed by sequential blotting of the same membrane without stripping (left panel). Relative protein levels were quantified using the ImageStudio program, with γ -tubulin for normalization (right panel). Representative of 2 independent experiments. **(G)** Summary

diagram of the reciprocal negative regulation of CSL and p53 expression and activity, respectively. As discussed in the text, in response to acute genotoxic/oxidative stress, such as UVA or ROS, p53 is activated and represses CSL, which is in turn not longer able to lessen p53 activity. Thus, CSL down-modulation allows for full p53 activation. * $p < 0.0001$, ** $p=0.0002$, *** $p=0.0006$, # $p=0.0089$, ## $p=0.0228$, ° $p=0.0024$.

Figure 1



I

Networks		pValue	Networks	pValue		
Inflammation	Complement system	3.483E-10	Cytoskeleton	Regulation of cytoskeleton rearrangement	2.899E-12	
Translation	Translation initiation	3.102E-06		Actin filaments	3.413E-11	
	Elongation- Termination	4.176E-03		Intermediate filaments	3.881E-09	
	Regulation of initiation	3.649E-02		Spindle microtubules	6.280E-04	
				Cytoplasmic microtubules	1.016E-03	
Proliferation	Positive regulation of cell proliferation	2.527E-03		Cell adhesion	Integrin-mediated cell-matrix adhesion	6.759E-12
	Negative regulation of cell proliferation	4.935E-02			Cell junctions	1.741E-06
Transport	Manganese transport	3.839E-03			Cadherins	8.947E-06
					Synaptic contact	4.143E-04
Development	Blood vessel morphogenesis	4.084E-02		Leukocyte chemotaxis	5.229E-04	
	Apoptosis	Anti-apoptosis mediated by external signals via NF- κ B	4.855E-02	Cell cycle	Mitosis	2.207E-06
			Meiosis		4.864E-04	
			Development	Neurogenesis_Axonal guidance	3.485E-05	
				EMT_Regulation of epithelial-to-mesenchymal transition	2.183E-04	
			Protein folding	Folding in normal condition	4.051E-04	
			DNA damage	DBS repair	1.097E-03	
			Immune response	Phagocytosis	1.328E-03	
				Phagosome in antigen presentation	1.508E-03	

J Transcription factors positively correlated to CSL

CSL	KLF3	PIAS1	ESR1
SP3	NFIL3	ZEB1	FOXP2
GPBP1	ARID4A	LPIN1	ZEB2
CREBL2	ZFP36L2	ING4	MED4
IFI16	OSR1	CREBRF	ATMIN
POLR2M	RBL2	MAF	MAX
CIR1	NDN	CNBP	TRIM22
TSHZ2	HBP1	LDB2	STAG2
PFDN5	PPARG	NR2C1	
BACH1	MSRB2	ZNF436	

Transcription factors negatively correlated to CSL

PRKDC	TAF6	MYBL2	TRIB3	NOC2L
FUBP3	SF1	NONO	HCFC1	AJUBA
ZNF789	MYBBP1A	SSRP1	PUF60	H2AFY
ZNF341	NOTCH1	CEBPG	SMARCD1	NCOR1
ARHGAP35	SRF	SNF8	TRIM24	SMARCA4
RBM14	PPRC1	MTA2	TEAD4	PUS1
ZNF202	ZFP69B	SMARCC1	WWP2	PDCD11
NPAS4	LOXL2	SMARCB1	FLNA	TGFB11
CAMTA2	PAWR	GATAD2A	WDR77	
TAF15	PTPN14	AFF3	DDX54	

Figure 2

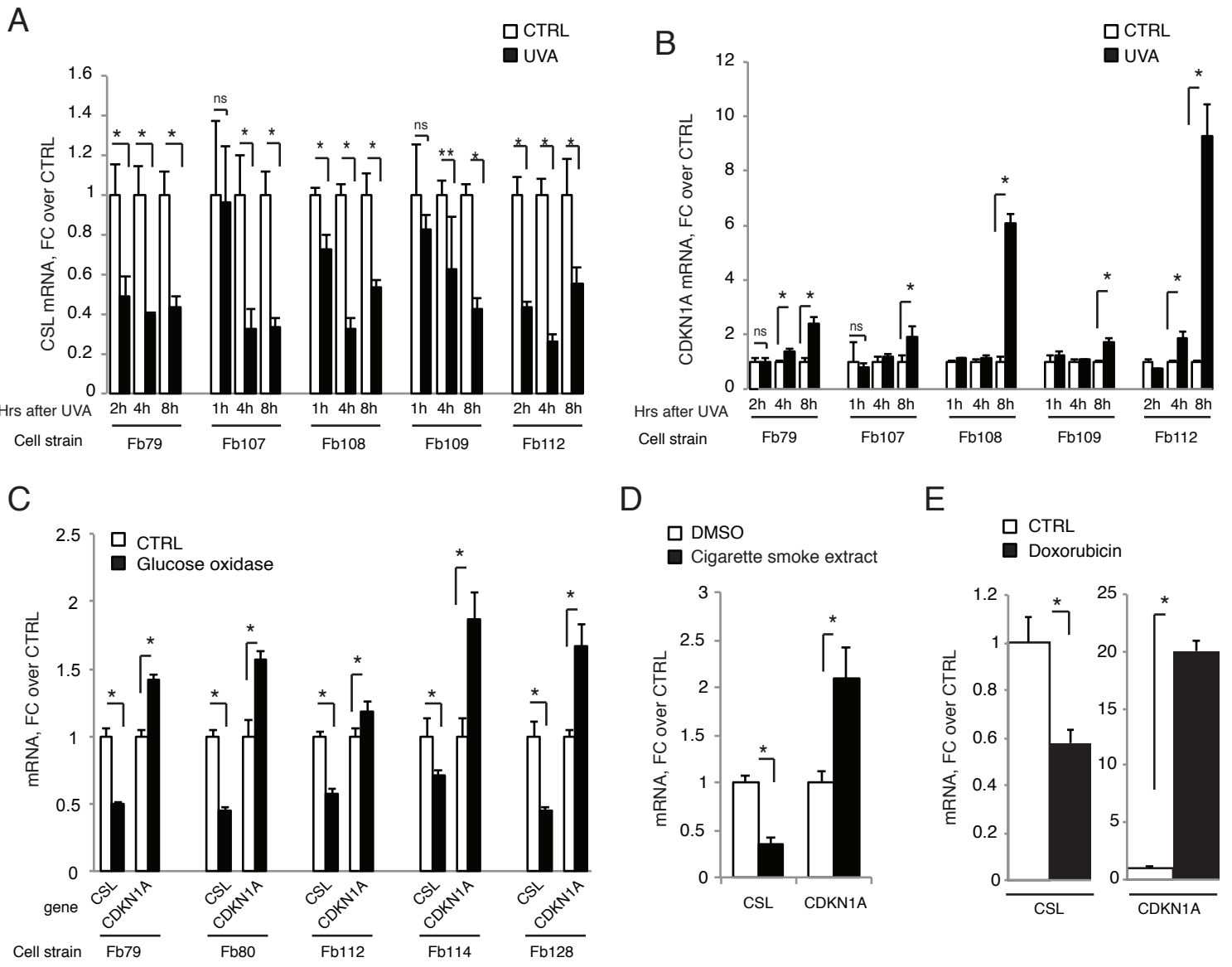
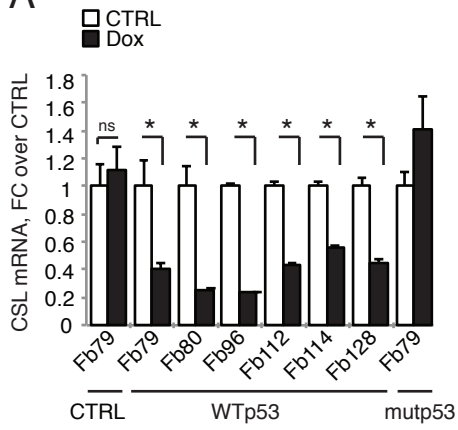
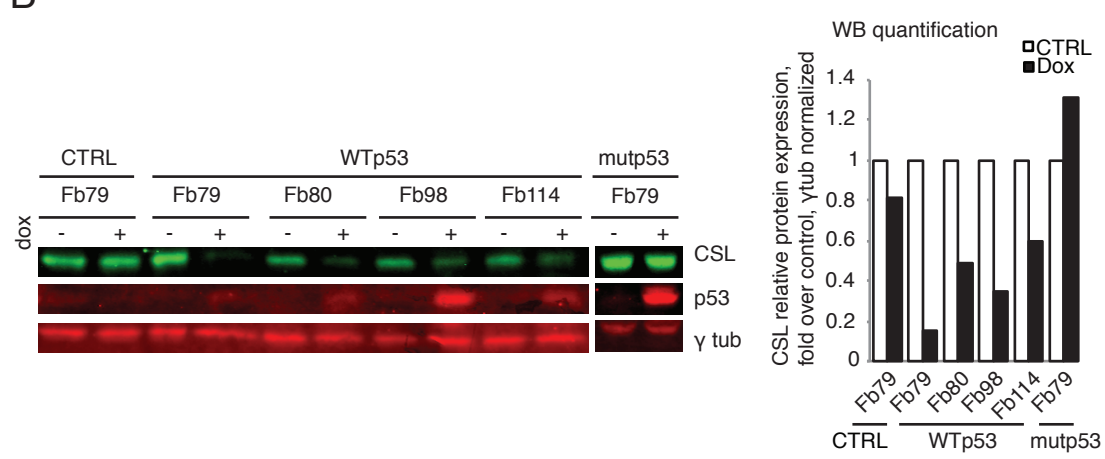


Figure 3

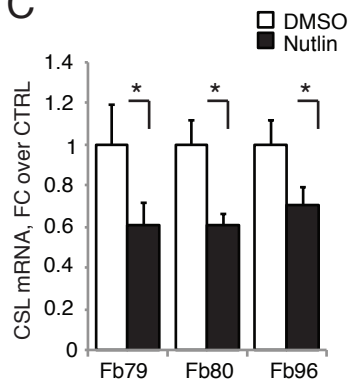
A



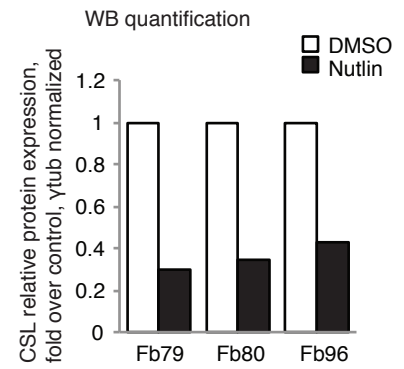
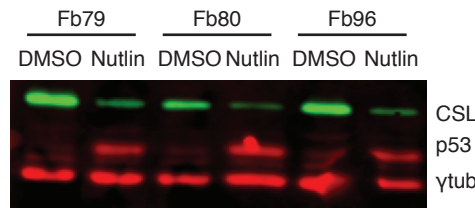
B



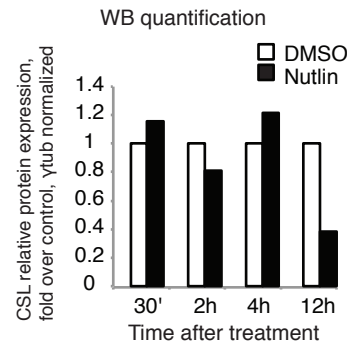
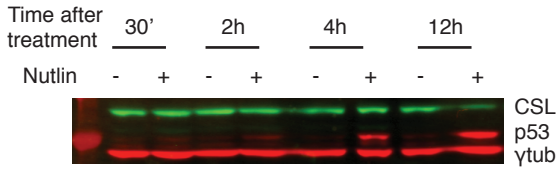
C



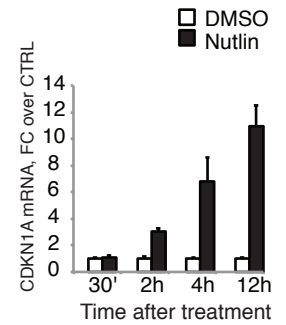
D



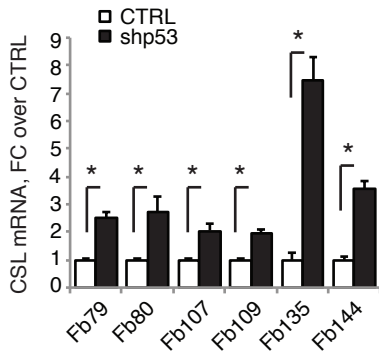
E



F



G



H

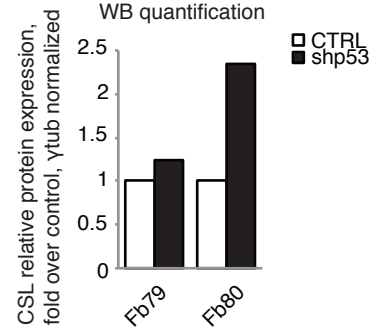
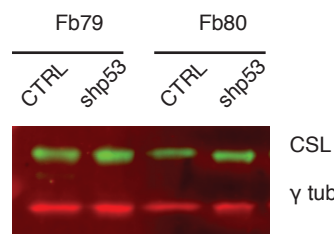
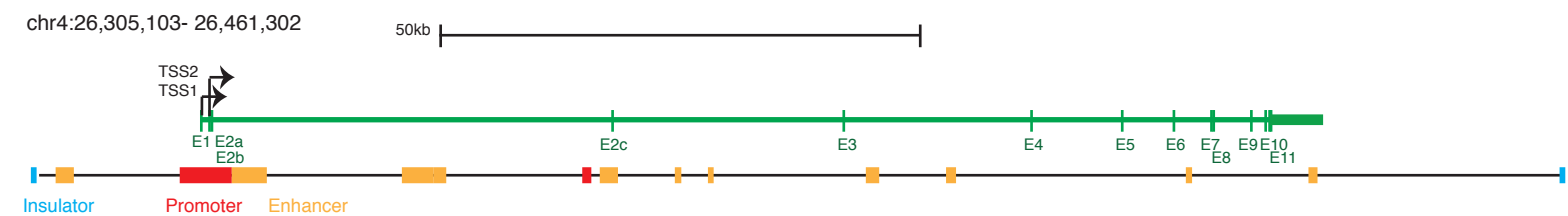
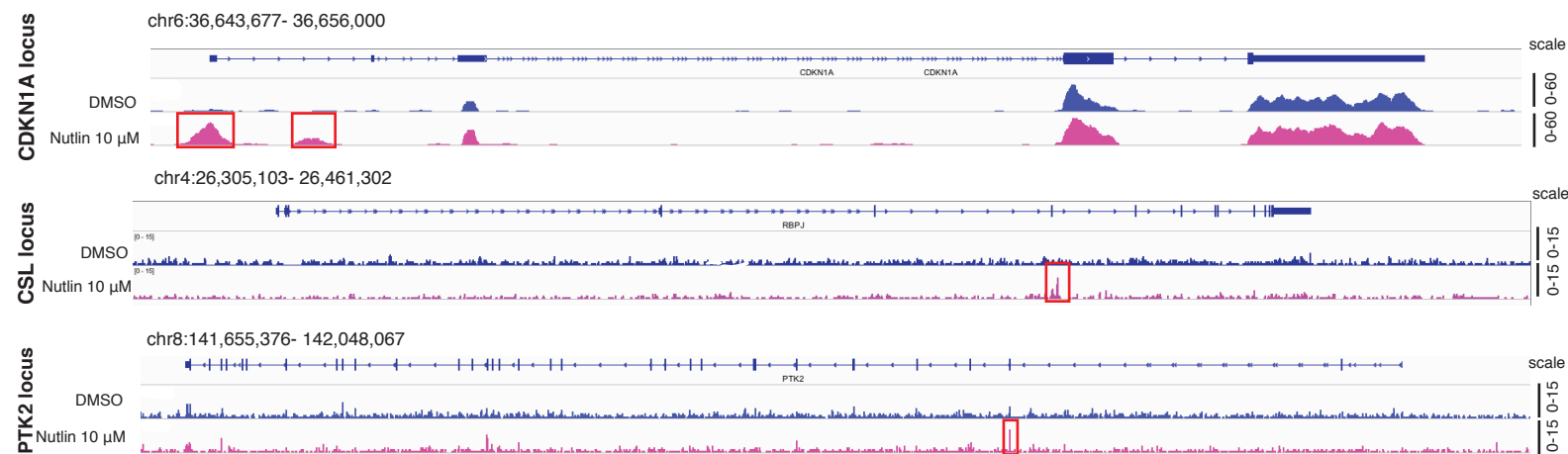


Figure 4

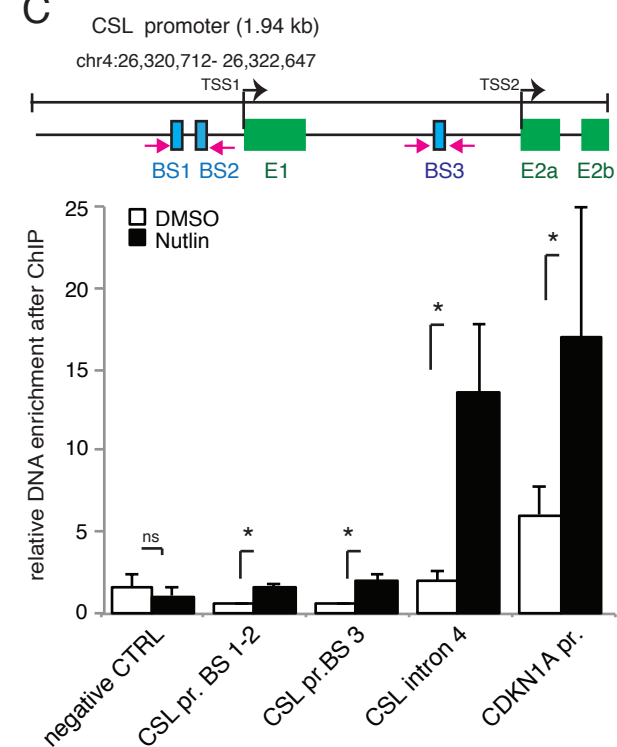
A



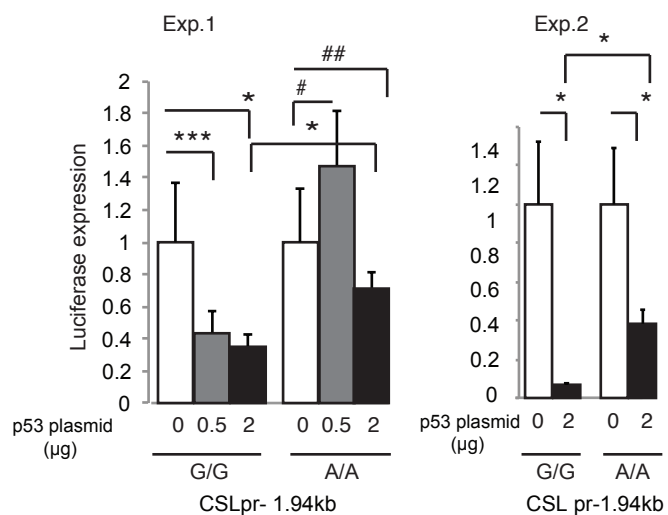
B



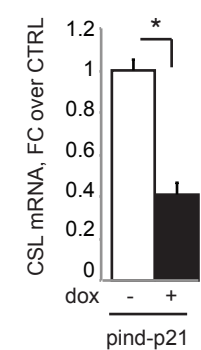
C



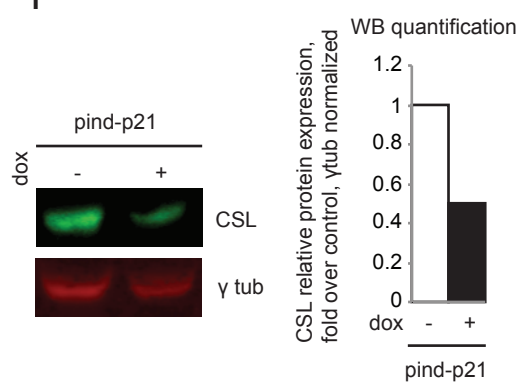
D



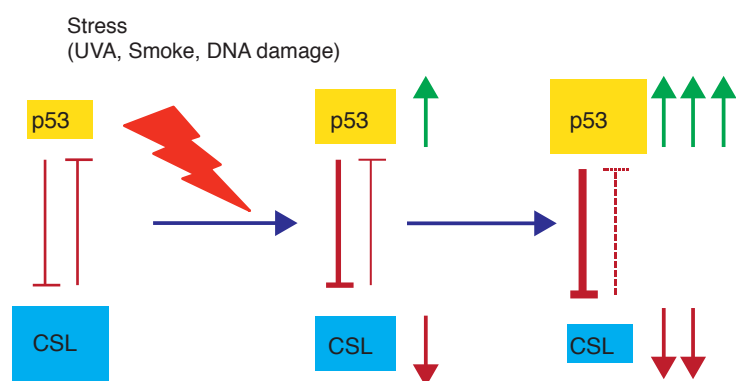
E



F

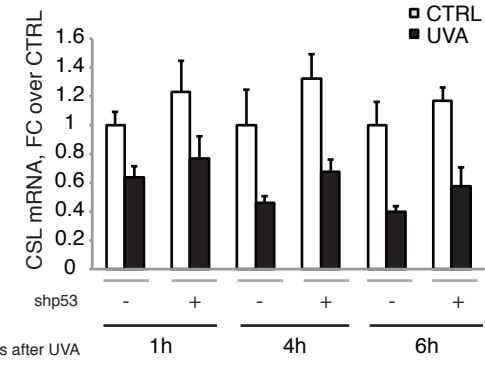


G

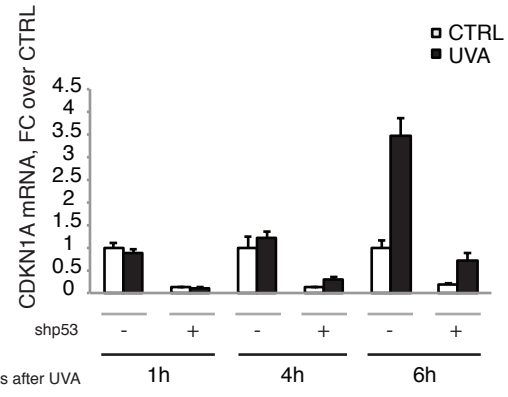
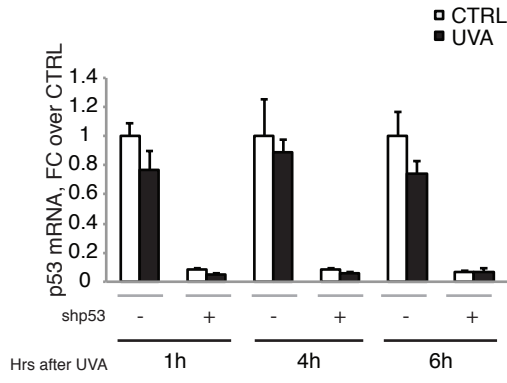


Supplementary Figure 1

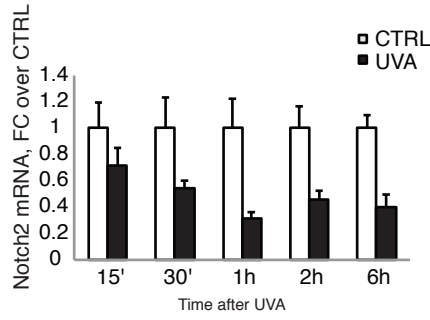
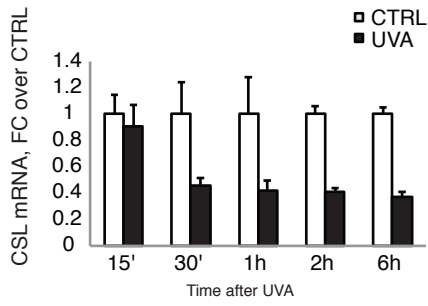
A



B



C



Supplementary Figure 1. P53 is not the main effector of UVA-induced CSL downregulation. (A,B) Human dermal fibroblasts (HDFs) stably infected with shRNA retroviruses against p53 in parallel with control viruses were irradiated with 1J/cm² of UVA, collected at the indicated time points and CSL (A), p53 and CDKN1A (B) mRNA levels were measured by RT-qPCR using 36β4 for normalization. **(C)** HDFs were treated with 1J/cm² UVA, collected at the indicated time points and CSL and NOTCH2 mRNA levels were measured by RT-qPCR using 36β4 for normalization.